

## METHOD

# recolorize: An R package for flexible colour segmentation of biological images

Hannah I. Weller<sup>1,2</sup>  | Anna E. Hiller<sup>3</sup> | Nathan P. Lord<sup>4</sup> | Steven M. Van Belleghem<sup>5</sup> 

<sup>1</sup>Department of Ecology, Evolution, and Organismal Biology, Brown University, Providence, Rhode Island, USA

<sup>2</sup>Helsinki Institute of Life Sciences, University of Helsinki, Helsinki, Finland

<sup>3</sup>Museum of Natural Science and Department of Biological Sciences, Louisiana State University, Baton Rouge, Louisiana, USA

<sup>4</sup>Department of Entomology, Louisiana State University Agricultural Center, Baton Rouge, Louisiana, USA

<sup>5</sup>Department of Biology, KU Leuven, Leuven, Belgium

### Correspondence

Hannah I. Weller, Viikinkaari 5, Room 6027b, 00790 Helsinki, Finland.  
 Email: [hannahiweller@gmail.com](mailto:hannahiweller@gmail.com)

### Funding information

National Science Foundation, Grant/Award Number: DEB 1841704 and DGE 2040433; Brown University

**Editor:** Greg F. Grether

### Abstract

Colour pattern variation provides biological information in fields ranging from disease ecology to speciation dynamics. Comparing colour pattern geometries across images requires colour segmentation, where pixels in an image are assigned to one of a set of colour classes shared by all images. Manual methods for colour segmentation are slow and subjective, while automated methods can struggle with high technical variation in aggregate image sets. We present recolorize, an R package toolbox for human-subjective colour segmentation with functions for batch-processing low-variation image sets and additional tools for handling images from diverse (high-variation) sources. The package also includes export options for a variety of formats and colour analysis packages. This paper illustrates recolorize for three example datasets, including high variation, batch processing and combining with reflectance spectra, and demonstrates the downstream use of methods that rely on this output.

### KEY WORDS

colour, colour pattern, image segmentation, R, software, trait analysis

## INTRODUCTION

Colour is an important source of biological variation, implicated in biological questions concerning development, genetics, thermal physiology, disease ecology and species identification, as well as sexual selection, animal communication and camouflage (Bates, 1863; Bekker et al., 1837; Hooper et al., 2020; Orteu & Jiggins, 2020; Poulton, 1890). Large comparative datasets of colour variation are generally necessary to investigate questions related to the developmental mechanisms of mimicry (e.g. Ezray et al., 2019; Marchini et al., 2017; Stuckert et al., 2021; Van Belleghem et al., 2020), hybridization (e.g. Medina et al., 2013; Miyazawa et al., 2010; Tea et al., 2020), parasite load (e.g. Houde & Torio, 1992; Megia-Palma et al., 2018; Ressel & Schall, 1989), polymorphism (e.g.

Brodie, 1992; Curlis et al., 2021; Gautier et al., 2018), or species identification (e.g. Jonathan, 1977; Parham et al., 2018). Often, the only practical way to collect these datasets is in aggregate: across multiple field seasons, localities, researchers, databases, or museums (e.g. Alfaro et al., 2019; Corbett et al., 2023; Robinson et al., 2023); but see van den Berg et al. (2023) or Dale et al. (2021) for examples of single-source datasets. This aggregation of images becomes especially problematic for taxa that do not retain their colour in preservation, including fish, amphibians and squamates. Uncalibrated digital images from community science databases like iNaturalist (Nugent, 2018) or the Macaulay Library at the Cornell Lab of Ornithology (<https://www.macaulaylibrary.org>) are the most common data type for measuring colour patterns in aggregate datasets (as of writing, iNaturalist

contains >96,000,000 research-grade observations with images and the Macaulay Library >50,000,000). These images provide valuable—and often irreplaceable—information for studying colour pattern variation in ecological contexts. For example, Laitly et al. (2021) found that images from community science databases can be used to measure colour variation by leveraging larger sample sizes of uncalibrated images. Accessing information from these kinds of datasets would expand our ability to quantitatively test predictions of colour pattern diversity (van den Berg et al., 2020).

Digital images capture a subset of light reflected from a surface using sensors optimized for human vision (see Stevens et al. (2007), especially the section on calibrating a digital camera). Unless they go through additional colour calibration steps, such as in micaToolbox in ImageJ (Troscianko & Stevens, 2015), uncalibrated digital images alone cannot be used to measure anything about how a colour pattern is perceived by a non-human observer (Johnsen, 2016). Such images cannot be used to compare chromatic (spectral) and achromatic (brightness and lightness) properties needed for visual modelling (Vorobyev & Osorio, 1998). However, human-subjective colour pattern geometry can be measured even from uncalibrated digital images, provided the relevant colour classes can be distinguished by a human viewer. These images thus still provide biologically relevant quantitative information (Figure 1).

For example, zebra species are identified by the distribution and spacing of their high-contrast stripes (Jonathan, 1977). If we were interested in how stripe spacing affects a biting fly's ability to gauge its distance to zebra skin when landing (Caro et al., 2019), we would have to model zebra colour patterns as biting flies would see them. If we were interested in how zebra stripes scale with body growth over development or whether stripes are more prevalent in regions with more biting flies (Caro et al., 2014), we could answer this question with uncalibrated images.

To compare colour patterns from uncalibrated images, we first need to identify homologous colour pattern elements across images. This process requires colour segmentation, which assigns each pixel in the region of interest to a discrete colour class as defined by the researcher, producing a *zone map* as first described by Endler (1984) and defined in Endler (2012) (Figure 1a–e). Crucially, a scientifically useful zone map has a biological justification for defining colour classes. These justifications may include, for example, the known pigment cell types of the colour classes (e.g. Kratochwil et al., 2018; Liang et al., 2020), taxonomic descriptions (e.g. Arbour et al., 2014; Brown et al., 2009; Leite & Mather, 2008), mathematical models of colour pattern establishment (e.g. Kondo & Asai, 1995; Miyazawa, 2020), or established heritability of ecologically important colour pattern elements (e.g. Sheehan et al., 2017).

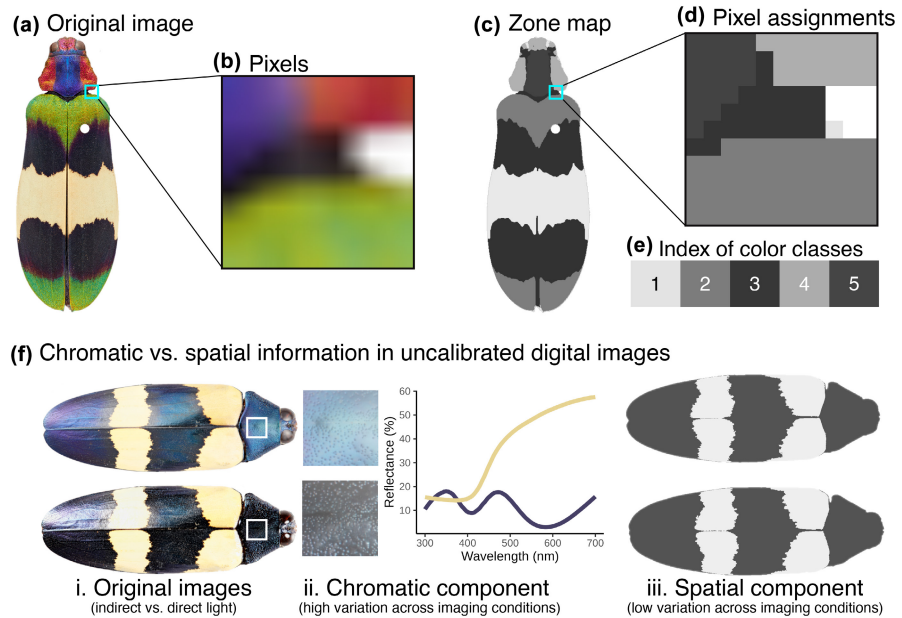


**FIGURE 1** An example of a zone map and distinguishing between spatial and chromatic components of colour patterns. (a) Original image of a beetle, *Chrysochroa corbetti* (Kerremans 1893). (b) Inset of individual pixels. (c) Zone map, where each pixel has been assigned to one of five colour classes. (d) The same inset from (b), where each pixel is assigned to a colour class. (e) The colour classes displayed as a colour palette. (f) Spatial components of colour patterns (as retained in a zone map) are more robust to imaging noise than chromatic components. i: The same specimen (*Chrysochroa mniszechii*, Deyrolle 1861), photographed using indirect (top) and direct (bottom) full-spectrum lighting. ii: The recorded RGB colour of the dark portion of the beetle's elytra changes with imaging conditions, even though the elytra's spectral properties remain the same, illustrating the unreliability of uncalibrated digital images for measuring chromatic data. iii: Zone maps created from each of the two images exhibit low variation (here differing by 1.5% of assigned pixels; see example code), illustrating that spatial components of colour patterns are more robust to imaging uncertainty.

Zone maps serve as a starting point for several R packages, including patternize (Van Belleghem et al., 2018), which quantifies colour pattern variation using a sampling grid; and the adjacent function in pavo (Maia et al., 2019), which outputs 16 summary colour pattern metrics including adjacency (Endler, 2012), boundary strength (Endler et al., 2018) and overall pattern contrast analyses (Endler & Mielke, 2005). Despite its general popularity in biological research, R lacks the same diversity of image segmentation tools as, e.g. Python (Bradski, 2000; Gollapudi, 2019) or MATLAB (MathWorks, 2023). R does have several image processing libraries, but many of these are focused on basic image processing steps (e.g. cropping, blurring, contrast/gamma adjustments; see Barthélémy and Tschumperlé (2019) or Ooms (2023)) or functions aimed at more general image segmentation tasks (e.g. identifying objects in a scene; Mouselimis (2023)). Having comparatively fewer tools in R for generating zone maps has hindered efficient analysis, particularly in cases of high variation across images (Figure 1f).

When generating zone maps, researchers can generally choose between automated, manual, or machine learning (ML) methods. Automated methods (Hartigan & Wong, 1979; Zhou, 2015) require little or no user input but are difficult to modify when they work poorly, while manual segmentation can be prohibitively slow (Menychtas et al., 2023). ML approaches require sufficient training data before they can be applied to biological questions, necessitating manual annotation (Laurence-Chasen et al., 2020; Mathis et al., 2018; Schwartz & Alfaro, 2021). Packages or other code for analysing biological colour in R sometimes provide a function for performing colour segmentation before running the rest of the intended analysis (e.g. watershedding in patternize). However, R users who need these zone maps for a purpose not implemented in that package need sufficient coding expertise to extract and modify them, especially from package-specific data structures (Maia et al., 2019; Schneider et al., 2012; Van Belleghem et al., 2018; Zhou, 2015).

We developed the recolorize R package as a flexible toolbox for colour segmentation that enables the use of downstream colour pattern analyses across uncalibrated datasets. The package requires (1) uncalibrated images and (2) a biological basis for user-defined colour classes that human viewers can identify in those images. The goal of this R package is to allow users to generate zone maps tailored to their specific research questions using a combination of automated and supervised functions. Datasets with less variation can be batch processed, while datasets with extreme variation that would have to be segmented manually can be processed in a faster, more reproducible way. We aim to make the package easy to use, easy to modify and easy to export to other packages (e.g. patternize and pavo) and workflows. We present three representative use cases involving supervised and automated functions, batch-processing a set of images with lower variation and the combination of zone maps with reflectance spectra for calibrating datasets

with extreme lighting variation. By implementing the recolorize package, we further enable quantitative colour pattern analysis in R and facilitate a more comprehensive understanding of colour pattern geometry across diverse organisms and datasets.

## GLOSSARY

The terms used for each of the components of this process vary somewhat in the literature; here we define their uses in this paper.

1. *Colour pattern*: Spatial variation in the spatiochromatic features of an animal's integument, per Kratochwil and Mallarino (2023).
2. *Colour pattern geometry*: The spatial component of a colour pattern.
3. *Colour class*: A specific ID (usually numeric) to which portions of the colour pattern are assigned.
4. *Colour centre*: The computer-readable colour of the colour class, typically an RGB triplet.
5. *Colour patch*: All the pixels in the image assigned to the same colour class.
6. *Colour space*: The 3D digital coordinate system used to represent the computer-readable colour of each pixel and/or colour class, as converted from the original RGB values of the input image without additional calibration (here restricted to sRGB, CIELAB, or HSV).
7. *Colour segmentation*: The process of segmenting an image into discrete colour patches.
8. *Zone map*: A numeric matrix assigning each pixel in an image to a colour class as the result of colour segmentation.

## METHODS

### Main recolorize toolbox

The recolorize package (version 0.1.0) offers several segmentation functions, rather than a single algorithm, but here we describe the tools used for a typical image segmentation.

First, each pixel in the image is assigned to a colour class in an initial binning step using the `recolorize` function. Rather than k-means clustering (an alternate method provided in the function), the default uses a histogram method, where pixels are assigned to a class based on ranges defined for each axis of colour space (Figure 2a). Users specify the number of bins per channel, where the total number of resulting colour centres is the product of the number of bins in each channel (e.g. 3 bins per channel yields  $3^3=27$  classes). The centre of each region is then calculated as the average value of all pixels assigned to that region (or the geometric centre if no pixels were assigned to it).

Second, the initial colour centres are reduced according to user-specified rules, such as combining

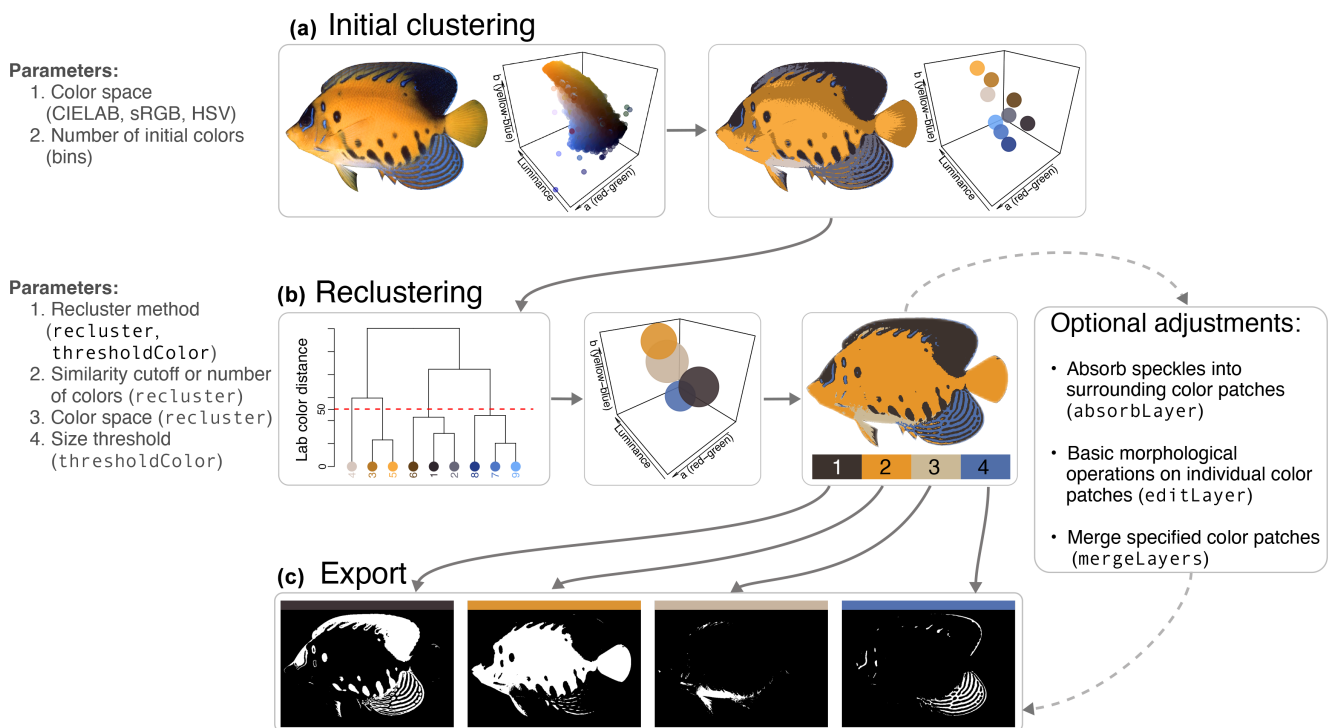


**FIGURE 2** Segmentation of a marine angelfish (*Pygoplites diacanthus*, Boddaert 1772) image, illustrating the core steps of the package. Parameters for each step are listed on the left. (a) First, the pixels of the original image are binned in each axis of colour space using a user-selected number of bins per channel using the `recolorize` function. (b) These initial bins are combined according to a rule, in this case distance in CIELAB space using `recluster`, by combining bins that have a Euclidean distance less than the user-selected cut-off (here,  $\text{cutoff}=50$ ). The original image is then re-fit using the resulting set of colour centres. (c) The resulting zone map is exported to any of a number of formats. Here, individual colour patches are exported as binary masks using the `splitByColor` function. Original image by Jack E. Randall via Bishop Museum, used under a CC BY-NC 3.0 licence.

similar colour centres (`recluster`) or dropping the smallest colour patches (`thresholdRecolor`) (Table 1). The most generally effective function for this step is the `recluster` function, which calculates the Euclidean distance between pairs of colours. Colour centres are then clustered by similarity using hierarchical clustering (R Core Team, 2022), and users provide either a similarity cut-off or a final number of classes. In Figure 2b, we used a cut-off of 50 (Euclidean distance in CIELAB colour space) to combine the 9 initial colour centres into 4 consensus colour centres. The `recluster` function then refits the original image with these new colour centres.

Third, if additional edits are needed, there are several functions for adjusting single layers or the resulting zone map as a whole. For example, specular reflections can be eliminated using the `absorbLayer` function. Other functions include basic morphological operations with `editLayer` and merging specified colour classes using `mergeLayer`. If users want to fit an image to an external set of colour centres (especially useful with batch processing), they can instead use only the `imposeColors` function, which fits an image to a supplied matrix of colour centres.

Finally, `recolorize` objects can be exported to any of several formats for downstream analyses. These

include a matrix indexed by colour class, recoloured images (`recolorize_to_png`), binary masks for each colour patch (`splitByColor`), lists of raster objects for use in the `patternize` package (version  $\geq 0.0.5$ , `recolorize_to_patternize`), `classify` class objects for use with the `pavo` package (version  $\geq 2.0$ , `classify_recolorize`), or vector images (`recolorizeVector`).

## Package installation, structure and input

### Installation

The most recent stable release version of the package can be installed from the Comprehensive R Archive Network (CRAN) in R (version  $\geq 3.50$ ) using the `install.packages()` function:

```
install.packages("recolorize")
```

The development version of the package can be installed from GitHub (<https://github.com/hiweller/recolorize>) using the `devtools` package (version  $\geq 2.4$ , Wickham et al., 2021):

```
devtools:::install_github("hiweller/recolorize")
```

**TABLE 1** Major functions of the recolorize package.

Function	Category	Description	Use
recolorize	Clustering	Clusters the pixels of an RGB image according to specified method	Initial colour clustering
recluster	Clustering	Cluster colour centres by distance in specified colour space	Combining similar colour classes in an over-clustered segmentation
recolorize2	Clustering	Calls the recolorize and recluster functions in sequence	Initial colour clustering
imposeColors	Clustering	Assign pixels to a provided set of colour centres	Batch processing; mapping a set of images to the same palette
thresholdRecolor	Toolbox	Reassign colour patches below a size threshold from a recolorize object	Dropping minor colour patches
absorbLayer	Toolbox	Absorb specified components of a colour patch	Handles specular reflections, uneven lighting
editLayer	Toolbox	Edit a colour patch using simple morphological operations	Removing speckles or filling holes in a colour patch
match_colours	Toolbox	Reorder colour centres to best match a reference palette	Batch processing; ensure that colour centres are in the same order across dataset
mergeLayers	Toolbox	Merge specified colour patches	Combining dissimilar colour classes where needed
reorder_colours	Toolbox	Reorder colour classes in a recolorize object	Batch processing; ensuring that colour centres are in the same order across images
classify_recolorize	Export	Convert a ‘recolorize’ object to a ‘classify’ object for the pavo package	Running adjacency analysis; combining with reflectance spectra
recolorizeVector	Export	Convert a recolorize object to a set of polygons	Visualization; rescaling zone maps
recolorize_to_patternize	Export	Convert a recolorize object to a list of RasterLayer objects for patternize	Running colour pattern PCA in patternize
rerun_recolorize	Export	Rerun functions used to produce a recolorize object	Reproducibility; applying the same series of calls to another image
splitByColor	Export	Generate a binary mask for each colour patch	Analyses that require region-of-interest (ROI) maps for each colour patch

## The recolorize class

The recolorize package mostly works with R objects of S3 class `recolorize`, which are output by the base functions and which most functions in later steps of the workflow will use as arguments. Objects of this class are lists with the following elements:

1. `original_img`: The original image, stored as a raster array (a matrix of hexadecimal codes).
2. `centers`: A matrix of colour centres, listed as one RGB triplet per row in a 0–1 range. These are usually the average colour of all pixels assigned to that colour class, unless otherwise specified by the user.
3. `sizes`: The number of pixels assigned to each colour class.
4. `pixel_assignments`: A matrix of colour class assignments for each pixel. For example, all pixels coded as 1 in the `pixel_assignments` matrix are assigned to colour class 1 (which will be row 1 of `centers`).
5. `call`: The set of commands that were called to generate the `recolorize` object.

The `call` object aids reproducibility because it stores every step used to generate the current segmentation (any function that returns a `recolorize` class object will modify the `call` element accordingly).

## RESULTS

All code and data required to run these examples are available at the following GitHub repository: [https://github.com/hiweller/recolorize\\_examples](https://github.com/hiweller/recolorize_examples) or on Dryad (DOI: 10.5061/dryad.9kd51c5r3).

### Example A: Aggregate dataset of highly variable images

The first example focuses on a set of uncalibrated images of *Neolamprologus* fish taken underwater at various depths and visibilities, which require human-subjective compensation for the lack of white balancing in the images that would otherwise necessitate manual

segmentation. The *Neolamprologus savoryi* (Poll 1949) complex of cichlid fishes has a diversity of facial colour pattern markings, which vary both between and within species (Gante et al., 2016) and are used to distinguish between individuals (Kohda et al., 2015). Because pigment patterns fade in preserved fish specimens (Neave et al., 2006; Poulsen et al., 2016), photographs of wild individuals are the best available data for facial colour pattern diversity in these fishes.

*Neolamprologus* colour patterns consist of three distinct pigment cell types: yellow xanthophores, blue iridophores and brown melanophores, providing a biological basis for colour segmentation (Bachmann et al., 2017; Santos et al., 2016). As cichlid visual systems are diverse and differ from those of humans (Carleton, 2009; Hofmann et al., 2009; Karagic et al., 2018), care should be taken when interpreting these results for perception.

Here, we analysed a set of images (courtesy of Ad Konings) of *N. brichardi* (Poll, 1974; Figure 3a, top two rows) and *N. pulcher* (Trewavas & Poll, 1952; Figure 3a,

bottom two rows), which occupy adjacent ranges and hybridize in the wild (Duftner et al., 2007). These images were taken at different depths, regions of Lake Tanganyika and times of day, resulting in the same set of pigment cells having substantially different RGB triplet values in each image. The goal of this example is to illustrate how the recolorize package can be used as a toolbox to perform segmentation on a per-image basis for datasets with high technical variation that inhibits the use of automated methods. This aggregate dataset exemplifies the challenges that recolorize aims to solve.

We compare standard k-means clustering, a modification of k-means clustering for batch processing, and recolorize. All clustering methods were implemented using recolorize (which includes k-means clustering) for consistency. In each case, images were first aligned to a uniform sampling grid using landmark alignment in the patternize package (Van Belleghem et al., 2018). After clustering, the zone maps generated by recolorize were converted to patternize objects using

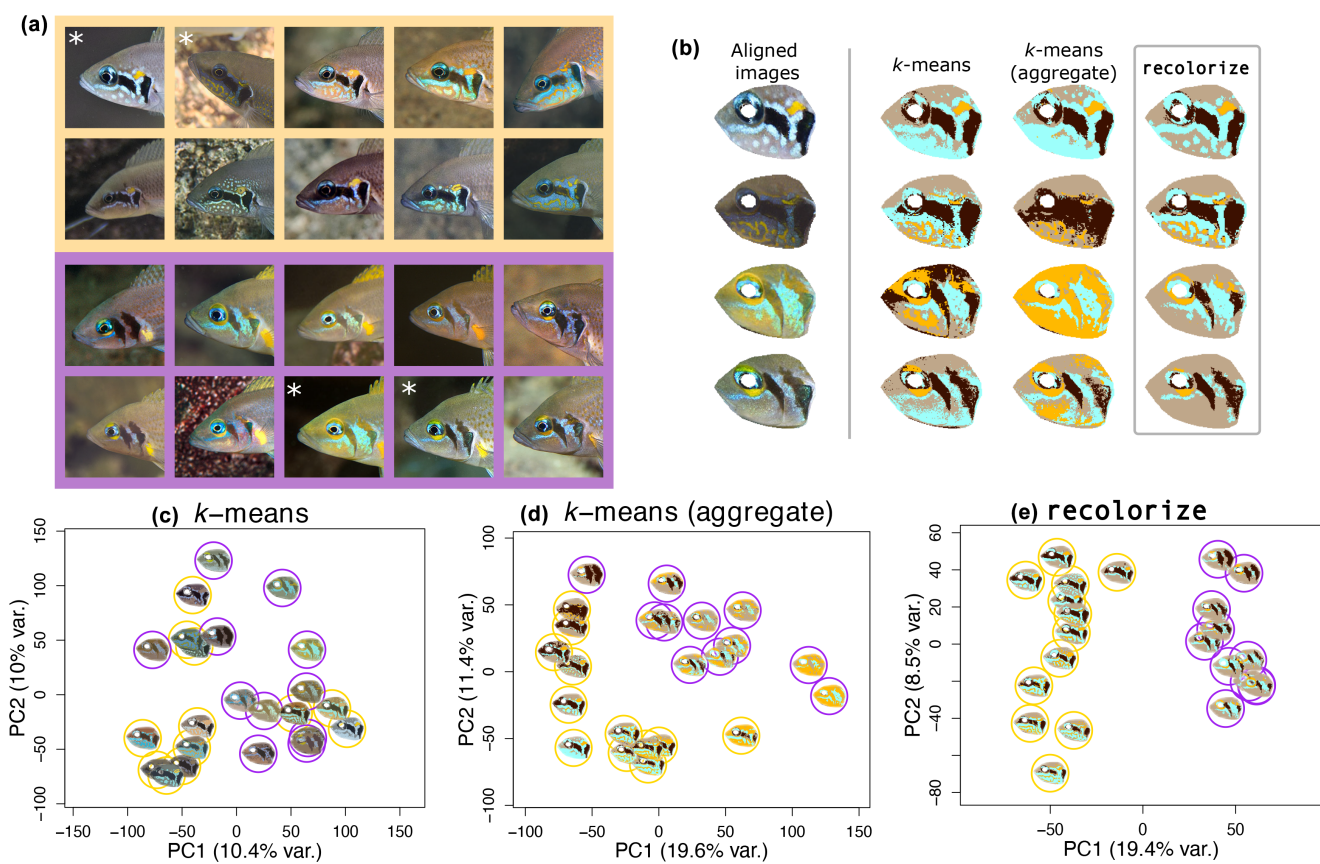


**FIGURE 3** Comparison of colour segmentation methods on an aggregate dataset of two *Neolamprologus* cichlid species, *N. brichardi* (yellow) and *N. pulcher* (purple). (a) Original field images, cropped to the head of each fish. *N. brichardi*, top two rows with yellow background; *N. pulcher*, bottom two rows with purple background. Despite facial colour patterns being composed of the same pigment cell types, their colours in the images vary with respect to camera, lighting, background and depth. Asterisks (\*) indicate images used as examples in (b). (b) Colour segmentation of four representative images (after landmark alignment with patternize). Segmentation methods were k-means clustering ( $n=4$  colours per image), aggregate k-means clustering (running k-means clustering on a combined image of all images), or recolorize. (c–e) PCA results using k-means (c), aggregate k-means (d), or recolorize (e). Original images by Ad Konings, used with permission.

`recolorize_to_patternize`, and a whole colour pattern principal components analysis (PCA) was conducted by treating each cell in the aligned images as a variable assigned to one of the colour classes (i.e. an  $n \times p$  array, where  $n$  is the number of images and  $p$  is the number of pixels in an aligned image; see example code).

Using standard heuristic k-means clustering, each image was clustered with  $n=4$  colours. Because unmodified k-means clustering is run independently for each image, the colour classes themselves vary across images and are inconsistent within an image across replicates (see supplement section 1.1). The resulting PCA does not separate the two species by their facial colour patterns (Adjusted Rand Index=0.021 comparing two-group clustering of Figure 3c and actual species identifications, where an ARI of 1 indicates clusters that match species identifications).

We also tried a modification of k-means clustering, which is to run the algorithm on all images simultaneously to identify a colour palette, then map each image to that set of colour centres using `imposeColors` (Figure 3b, third column, and d). In the four example images we show in Figure 3b, the blue iridophore patch is almost entirely lost in the second image, and in the third, almost the entire head is assigned to the yellow xanthophore colour class because of the greenish tinge to the image. The resulting PCA has better clustering than unmodified k-means, but still does a poor job of recovering the original species identifications (ARI=0.29), while still providing different results depending on the replicate (supplement section 1.1).

We used `recolorize` to perform initial colour segmentation for all images using the base `recolorize` function followed by `thresholdRecolor`. While image datasets with less extreme variation can be processed by `recolorize` using only one or two functions applied across the full dataset, here we provided different parameters for each image. This required processing using up to three additional functions from `recolorize`, such as `mergeLayers` to combine specified colour patches regardless of colour similarity, `absorbLayer` to reduce speckling, or `reorder_colours` to order the colour patches uniformly across images (see Figures S1 and S2; Table S1 for examples and details).

All edits are recorded in the call element of each `recolorize` object for reproducibility, meaning that the zone map can always be regenerated from the original. These edits can also be accessed in the example dataset. While this is slower than batch processing with a single function, `recolorize` produces usable results without requiring manual segmentation. The resulting PCA separates the two species entirely on PC1 (Figure 3e), and accordingly, hierarchical clustering on the PCA produced two groups that exactly match the species identifications (ARI=1). As this process can produce greater per-user variation than batch

processing, we segmented the dataset two additional times (once from the same user, once from a different user) and found an average of 11.7% of pixels assigned differently across users, largely at the margins of the colour patches, but with the two species still successfully separating on PC1 for each replicate (supplement section 2.1, Figure S2).

## Example B: Batch-processing for uniform images

With a set of images taken under more controlled conditions, `recolorize` can batch process images. Here we show an example using twenty *Polistes fuscatus* (Fabricius 1793) social wasp face images (Figure 4a) used with permission from the original set of 267 in Tumulty et al., (2023). The goal of the original paper was to illustrate a latitudinal gradient of facial colour pattern diversity that may relate to social behaviour. Here, the human-viewable colour classes are defined by their previously established heritability (Sheehan et al., 2017): black, brown and yellow.

Prior to analysis, images were normalized for luminance using reflectance standards (90%, 27% and 3% reflectance: Colour-aid grey set) and exported in sRGB colour space using `micaToolbox` (Troscianko & Stevens, 2015). As in example A, images were aligned and transformed to the sample mean shape via landmark alignment using the `alignLan` function in `patternize`. Next, we ran `recolorize` and `recluster` on each image individually to generate a colour palette for each image, and combined all palettes into a larger list of colours from which we extracted an aggregate palette of three colours using `hclust_color` (Figure 4b). We mapped each original image to this colour palette using `imposeColors` and performed a whole-colour-pattern PCA as in Example A (Figure 4d). The entire colour segmentation process in this case took 2–4 min and illustrated a northern to southern gradient of facial colour patterns in wasp populations (Tumulty et al., 2023).

## Example C: Combining images with reflectance spectra

While RGB images can be used to analyse colour pattern geometry, as in the previous two examples, the pixel colours in the images can vary drastically depending on the lighting and photography conditions. For example, Figure 5a,b feature the same two *Diglossa* bird specimens photographed under four combinations of camera, lighting and photography settings. This variability could technically be mitigated through colour calibration (Stevens et al., 2007; Troscianko & Stevens, 2015; van den Berg et al., 2020), but the required calibration references are often not included in aggregated image sets. This example illustrates how combining zone maps and spectra

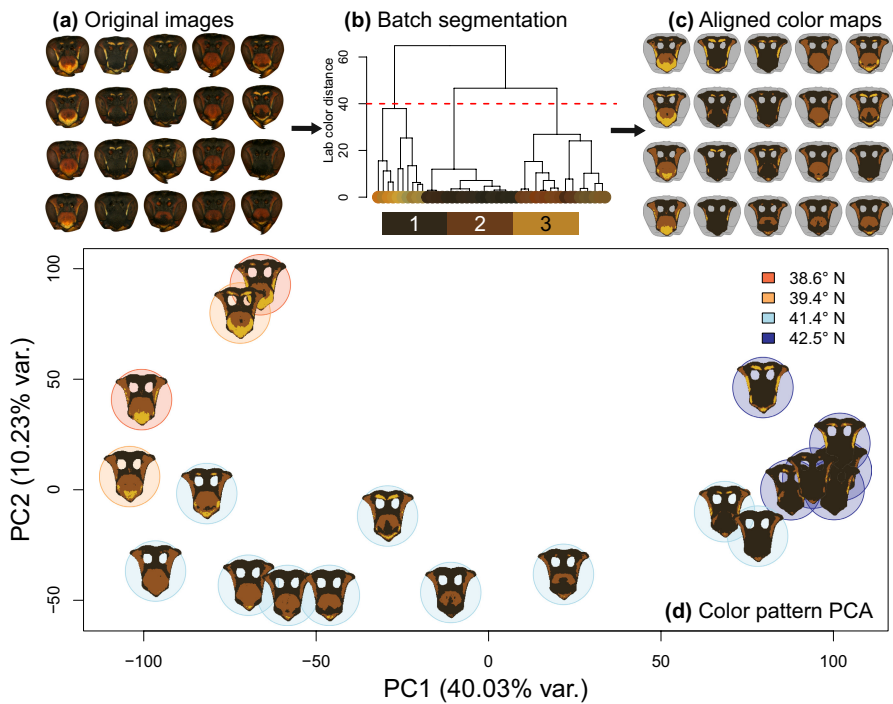


**FIGURE 4** Batch processing example using *Polistes fuscatus* wasps. (a) Original images of *Polistes fuscatus* wasp faces, taken with the same lighting and camera conditions. (b) Generating a single colour palette from colour segmentation on individual images. (c) Applying the colour palette using the `imposeColors` function to generate zone maps. (d) Colour pattern PCA as generated by aligned and segmented images, characterizing colour pattern diversity among the wasp face images. Coloured circles behind wasp zone maps indicate the latitude at which each specimen was collected for photography. Images by James Tumulty, used with permission and reproduced from Tumulty et al. (2023).

can provide much more reliable information than analysing images alone when the imaging conditions are unknown or cannot be calibrated.

One proposed solution for uncalibrated images is to combine zone maps, which provide spatial information from uncalibrated images, with reflectance measurements taken with a point spectrometer. This method has previously been described by Endler (1990); Endler and Houde (1995); Endler and Mielke (2005) and Winters et al. (2018) and is implemented in the `adjacent` function in the `pavo` package (Endler, 2012; Endler et al., 2018; Endler & Mielke, 2005; Maia et al., 2019). This can be especially helpful in cases where photographs are uncalibrated but reflectance spectra are available, e.g. photographs of wild individuals and reflectance spectra from museum or captive specimens. However, note that this is only appropriate when (1) repeated measurements indicate that the spectral properties of these colour patches are consistent across individuals, and (2) researchers can make the simplifying assumption that point spectra are representative of a colour patch as segmented in an uncalibrated image.

To illustrate how this process can allow users to capture the same colour information from photographs taken under different conditions, we calculated the average luminance of the images in Figure 5a,b for a human visual system using two methods: (1) from the pixel RGB values, and (2) by combining zone maps and spectra. We chose to model a human viewer because RGB images are meant to

approximate human vision, as is CIELAB colour space (Janos, 2007), making this the most appropriate visual system for comparing to the image pixel analysis.

We first processed bird images through patternize, as in Example B, to control for shape variation. To calculate luminance directly from images, we converted the RGB pixels of each processed image (without segmentation) to CIELAB colour space using a D65 reference illuminant and took the average of the luminance ( $L$ ) coordinate for every pixel in an image. This approach represents the outcome of using image RGB colours as the basis for comparing achromatic values across uncalibrated images.

To calculate luminance using a combination of zone maps and spectra, we segmented the landmark-aligned images using recolorize and converted the zone maps to classify objects using `classify_recolorize` (Figure 5d,f). Flowerpiercers exhibit striking yet minute colour pattern repetition within and between species (Remsen Jr, 1984; Vuilleumier, 1969). Like many birds, their feathers can create irregular shadows and specular reflections that become more apparent under certain photography conditions and interfere with colour segmentation (Mason & Bowie, 2020).

We calculated hue-saturation-luminance (HSL) coordinates for point spectra from each colour patch (Figure 5c,e) for a human trichromatic visual system (see supplement section 2 for reflectance spectra collection procedure). We first calculated relative quantum

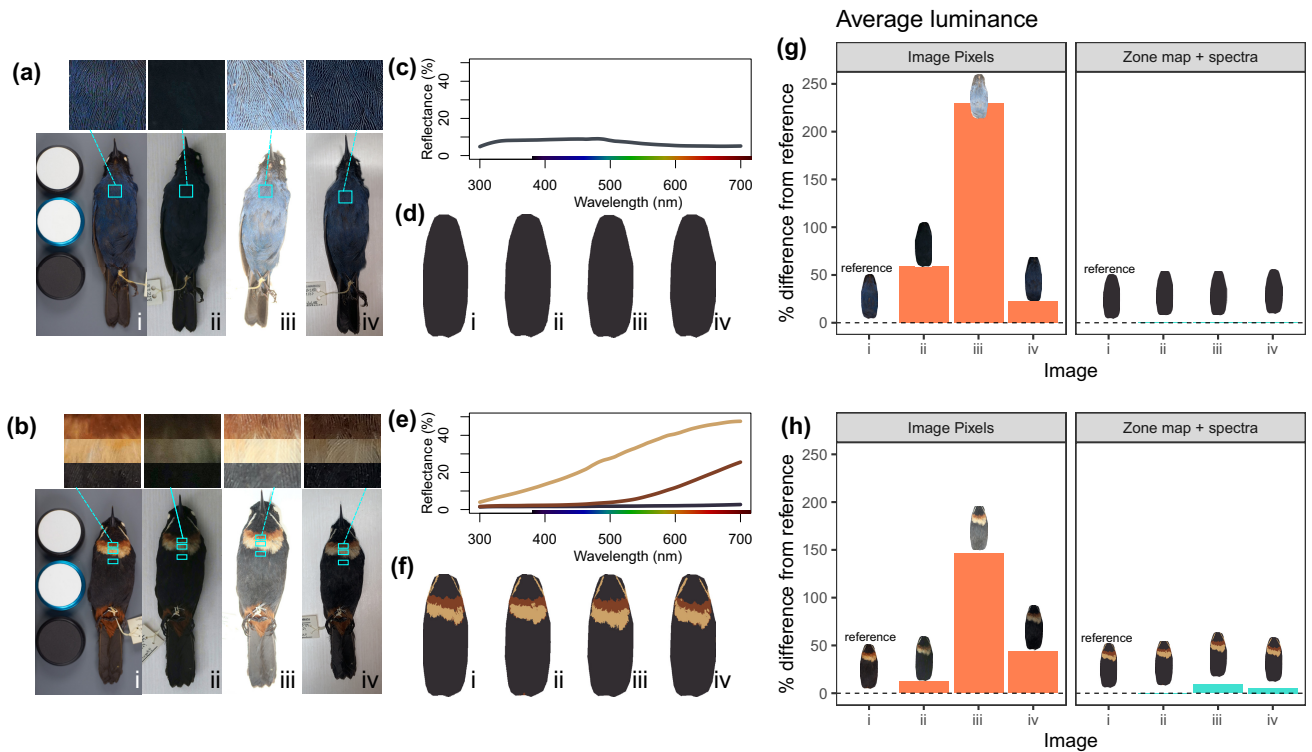


**FIGURE 5** Combining zone maps with spectral data in *pavo*. (a, b) Images of the same birds (a: LSUMZ 196409; b: LSUMZ 129286) taken under a variety of lighting conditions and camera settings. i: Nikon D7000 camera with full-spectrum quartz conversion and Novoflex Noflexar 35 mm lens – Calibrated VIS (RGB), ISO 400, shutter speed 1/1000s, full-spectrum light bulbs. ii: Canon 80D normal DSLR not calibrated – no flash, no lights on/dim room, F8.0, shutter speed 1/50s, ISO 2000, exposure +1. iii: Canon 80D normal DSLR not calibrated – with flash, overhead fluorescent lights on, F5.6, shutter speed 1/160s, ISO 500, exposure +2. iv: iPhone XR phone camera not calibrated – with flash, overhead fluorescent lights on. Insets for each image highlight the same patch (a) or patches (b) that were measured with the spectrometer, shown side-by-side to illustrate colour differences across the images. (c and e) Spectra for each of the patches in (a) and (b). (d and f) Zone maps for each of the images in (a) and (b). (g, h) Average luminance (using the average of the medium- and long-wavelength cones for a trichromatic human viewer) as calculated by the adjacent function in *pavo*, with colours calculated from image pixels on the left and from combining the zone map and spectra on the right. For each case, we show the difference in calculated luminance from the calibrated reference image taken under full-spectrum lighting with grey standards (image i).

catch values using the `vismodel` function in *pavo* using human spectral sensitivities (Stockman & Sharpe, 2000). We calculated luminance (achromatic) receptor stimulation by averaging the summed response for the medium- and long-wavelength photoreceptors (Eisner & MacLeod, 1980; Guth et al., 1968). We converted these quantum catch values to coordinates in a trichromatic colour space using *pavo*'s `colspace` function (see GitHub code and supplement section 2 for visual modelling details). We then analysed each image using the `adjacent` function in *pavo*, which (among 15 other metrics) calculates the mean pattern luminance of the segmented image by taking the average luminance of the provided colour space coordinates weighted by their relative size in the segmented image (Maia et al., 2019). This mean pattern luminance is comparable to the mean luminance calculated directly from the pixel RGB values in that both are intended to summarize the achromatic intensity of the bird as it would appear to a human observer under standard daylight conditions.

We calculated the difference between the luminance from the reference image (image i in Figure 5a,b), which

was taken with full-spectrum lights and calibrated using three Spectralon reflectance standards (5%, 80% and 100%) and each subsequent image. Combining the zone map and spectra provided nearly identical luminance values across all four images in both cases, while the results using the image pixels differed substantially (Figure 5g,h). Images of the first specimen (LSUMZ 196409, *Diglossa cyanea*) differed from the reference value by 22.3% to 229.9% (mean of 103.6%) using the image pixels. Using the zone map and spectra, differences from the reference image were much lower and ranged from 0.6% to 0.9% (mean of 0.7%). The second specimen (LSUMZ 129286, *Diglossa mystacalis*) scored similarly: 12.1% to 146.3% (mean of 67.3%) difference for the image pixels, and 0.3% to 10.4% (mean of 5.1%) difference for zone map and spectra. The colour pattern geometry measured in each image was highly consistent and could be reliably paired with spectra to produce results with low variation. Note that the sources of variation for the pixel and zone map/spec- tra results are different. For the pixel analyses, variation comes from the lack of image calibration. For the zone map/spec- tra analyses, the observed variation comes from

differences between the zone maps generated for each image because we use the same spectra for each image.

## DISCUSSION

We demonstrate how the recolorize package provides a flexible toolbox for human-subjective colour segmentation, which is appropriate when (1) there is a biological justification for defining the colour patches to segment, and (2) the colour patches are visible to human viewers. In these cases, recolorize strikes a balance between fully automated methods (which are difficult to modify when they do not work well) and fully manual methods (which are labour-intensive). In the simplest case, users only tinker with the number of initial colour centres in the first step and the similarity cut-off in the second step. In more complicated cases, which would otherwise be segmented manually, zone maps are modified and their code recorded in the call element of the recolorize objects. This allows recolorize to handle a wide range of colour segmentation problems, as demonstrated in our examples of three different taxa (fish, insects and birds).

Perhaps the trickiest part of using the package is defining the colour classes so that the human-subjective segmentation can be done to a consistent standard. This package specifically enables the user to produce subjectively suitable segmentations according to externally defined criteria, which is only scientifically valid if the user has a clear biological basis for colour classes. Otherwise, users may rely on aesthetic taste to produce zone maps that provide little biological information.

## Complementarity with existing methods

Because recolorize is a dedicated package for making zone maps, it is designed not as a replacement for existing colour pattern analyses but as a complement to them. By making colour segmentation more feasible and providing export options, recolorize makes other colour analysis tools easier to use for a wider variety of datasets.

Here, we compared recolorize to various implementations of k-means clustering because this is by far the most comparable method in terms of implementation in existing packages. We also compared the package to two other colour segmentation tools (supplement section 3, Figure S3) as a useful reference for users surveying options for colour segmentation, to illustrate the cases in which recolorize is the most appropriate tool (Zhou, 2015). By providing export options to the pavo and patternize packages, as well as more general export options for images, vector graphics and binary masks for individual layers, we aim to make the output of this package easy to integrate with other analyses.

## Integration with spectral data

Example C used a human visual system model to illustrate the light- and camera-dependence of the colours in uncalibrated images, and thus their unreliability for colour measurements. In theory, this same approach of combining zone maps and spectra to acquire both the spatial and chromatic aspects of a colour could be used with non-human visual systems, but only if prior research has shown that the relevant colour segmentation for the non-human visual system can be reliably produced by a human user. Parameters such as visual acuity and the number, ratio and spectral sensitivities of cone cell types vary widely across animal visual systems (Endler et al., 2005), meaning that the same colour pattern can be perceived entirely differently by two observers. This is evident even between humans, where the red-green chromatic contrast that appears bright to a trichromatic individual is greatly reduced for red-green colourblind individuals (Graham & Hsia, 1958; Saysani et al., 2018). It is therefore never reasonable to assume that the colour classes that seem obvious to a human viewer of a digital image would be perceived as such by a non-human viewer in the wild, or that a surface that appears uniform to a human viewer does not have important variation for a non-human viewer. However, in cases where RNL clustering of calibrated images for a non-human visual system (analysed with, e.g. QCPA; van den Berg et al., 2020) can also be distinguished by a researcher in an RGB image, one could use recolorize to analyse uncalibrated images using this classification scheme.

## Current and potential applications for recolorize

### Training for machine learning

Recolorize stores the exact set of calls used to generate individually edited zone maps for variable datasets, which means the package improves upon editing a zone map by hand (in terms of reproducibility). An ideal solution would require no individual interference. One possibility would be to use recolorize to generate a training set for machine learning approaches. Performing segmentation in recolorize can speed up the process of generating training data, so machine learning approaches could be used for more specific problems.

### Other potential uses of recolorize

Currently, recolorize works with the common image formats of PNG and JPEG images. The underlying package structure can be easily extended to other formats as the central algorithms of the package can be modified to images with more than 3 channels, and intermediate steps are exported as their own functions. For example, we

recently used recolorize functions for colour segmentation of 3D objects (STL file output from photogrammetry; Christopher Taylor, pers. comm.). It will be similarly straightforward to add existing image segmentation tools, either as available in R or integrated with OpenCV (Bradski, 2000; Eddelbuettel & Balamuta, 2018). Such future developments, often driven by specific user cases, will be made available on GitHub.

## AUTHOR CONTRIBUTIONS

HIW wrote the package, example code and manuscript. NPL provided images, feedback, funding and edited the manuscript. AEH provided bird data (images and spectra) and helped write the manuscript. SVB helped with package compatibility, contributed to the examples and edited the manuscript.

## ACKNOWLEDGEMENTS

We are grateful to Ad Konings, James Tumulty, Alison Davis-Rabosky and Able Chow for providing images. Christopher Taylor, Ghislaine Cardenas-Posada, Matthew Fuxjager, John Capano and Nicole Moody provided helpful feedback on the first draft of the paper. Sandra Winters provided advice for the examples in the paper. Elizabeth Karan and Shawn Shwartz provided early feedback on the package structure. Thank you to the Louisiana State University (LSU) colour seminar group and Brant Faircloth for sparking the discussions that led to this paper. Thanks to Robb Brumfield, Nick Mason and the LSU Museum of Natural Science for access to and resources for photographing bird specimens. Elizabeth Brainerd provided HIW the academic freedom to pursue this project. We would especially like to thank Jolyon Troscianko, Cedric van den Berg and an additional anonymous reviewer for their valuable feedback on earlier versions of the manuscript.

## CONFLICT OF INTEREST STATEMENT

The authors declare no competing interests.

## PEER REVIEW

The peer review history for this article is available at <https://www.webofscience.com/api/gateway/wos/peer-review/10.1111/ele.14378>.

## DATA AVAILABILITY STATEMENT

The development version of the package is available on GitHub: <https://github.com/hiweller/recolorize>. The stable release version is available on the Central R Archive Network: <https://cran.r-project.org/package=recolorize>. All images and code used to generate the examples are available in a separate Github repository: [https://github.com/hiweller/recolorize\\_examples](https://github.com/hiweller/recolorize_examples).

## ORCID

Hannah I. Weller  <https://orcid.org/0000-0002-5252-4282>

Steven M. Van Belleghem  <https://orcid.org/0000-0001-9399-1007>

## REFERENCES

- Alfaro, M.E., Karan, E.A., Schwartz, S.T. & Shultz, A.J. (2019) The evolution of color pattern in butterflyfishes (Chaetodontidae). *Integrative and Comparative Biology*, 59(3), 604–615. Available from: <https://doi.org/10.1093/icb/icz119>
- Arbour, J.H., Salazar, R.E.B. & López-Fernández, H. (2014) A new species of *Bujurquina* (Teleostei: Cichlidae) from the Río Danta, Ecuador, with a key to the species in the genus. *Copeia*, 2014(1), 79–86. Available from: <https://doi.org/10.1643/CI-13-028>
- Bachmann, J.C., Cortesi, F., Hall, M.D., Marshall, N.J., Salzburger, W. & Gante, H.F. (2017) Real-time social selection maintains honesty of a dynamic visual signal in cooperative fish. *Evolution Letters*, 1(5), 269–278. Available from: <https://doi.org/10.1002/evl3.24>
- Barthélémy, S. & Tschumperlé, D. (2019) Imager: an R package for image processing based on CImg. *Journal of Open Source Software*, 4(38), 1012. Available from: <https://doi.org/10.21105/joss.01012>
- Bates, H.W. (1863) *The naturalist on the river amazons*. London, UK: John Murray.
- Bekker, I., Sylburg, F. & Neumann, K.F. (1837) *Historia animalium. E Typographeo academico*. <https://books.google.com/books?id=2Z8NAAAAYAAJ>
- Bradski, G. (2000) The openCV library. *Dr. Dobb's Journal: Software Tools for the Professional Programmer*, 25(11), 120–123.
- Brodie, E.D. (1992) Correlational selection for color pattern and antipredator behavior in the garter Snake *Thamnophis ordinoides*. *Evolution*, 46(5), 1284–1298. Available from: <https://doi.org/10.1111/j.1558-5646.1992.tb01124.x>
- Brown, R.M., Siler, C.D., Diesmos, A.C. & Alcala, A.C. (2009) Philippine frogs of the genus *Leptobrachium* (Anura; Megophryidae): phylogeny-based species delimitation, taxonomic review, and descriptions of three new species. *Herpetological Monographs*, 23(1), 1–44.
- Carleton, K. (2009) Cichlid fish visual systems: mechanisms of spectral tuning. *Integrative Zoology*, 4(1), 75–86.
- Caro, T., Argueta, Y., Briolat, E.S., Bruggink, J., Kasprowsky, M., Lake, J. et al. (2019) Benefits of zebra stripes: behaviour of tabanid flies around zebras and horses. *PLoS One*, 14(2), e0210831.
- Caro, T., Izzo, A., Reiner, R.C., Jr., Walker, H. & Stankowich, T. (2014) The function of zebra stripes. *Nature Communications*, 5(1), 3535.
- Corbett, E.C., Brumfield, R.T. & Faircloth, B.C. (2023) The mechanistic, genetic and evolutionary causes of bird eye colour variation. *Ibis*, 165, ibi.13276. Available from: <https://doi.org/10.1111/ibi.13276>
- Curlis, J.D., Davis Rabosky, A.R., Holmes, I.A., Renney, T.J. & Cox, C.L. (2021) Genetic mechanisms and correlational selection structure trait variation in a coral snake mimic. *Proceedings of the Royal Society B*, 288(1947), 20210003.
- Dale, K., Hallisey, R. & Mehta, R. (2021) Coloration is related to habitat in *Gymnothorax mordax*, a kelp forest predator. *Marine Ecology Progress Series*, 677, 67–79. Available from: <https://doi.org/10.3354/meps13873>
- Duftner, N., Sefc, K.M., Koblmüller, S., Salzburger, W., Taborsky, M. & Sturmbauer, C. (2007) Parallel evolution of facial stripe patterns in the *Neolamprologus brichardi/pulcher* species complex endemic to Lake Tanganyika. *Molecular Phylogenetics and Evolution*, 45(2), 706–715. Available from: <https://doi.org/10.1016/j.ympev.2007.08.001>
- Eddelbuettel, D. & Balamuta, J.J. (2018) Extending extitR with extitC++: a brief introduction to extitRcpp. *The American Statistician*, 72(1), 28–36. Available from: <https://doi.org/10.1080/00031305.2017.1375990>

- Eisner, A. & MacLeod, D.I.A. (1980) Blue-sensitive cones do not contribute to luminance. *Journal of the Optical Society of America*, 70(1), 121. Available from: <https://doi.org/10.1364/JOSA.70.000121>
- Endler, J.A. (1984) Progressive background in moths, and a quantitative measure of crypsis. *Biological Journal of the Linnean Society*, 22(3), 187–231. Available from: <https://doi.org/10.1111/j.1095-8312.1984.tb01677.x>
- Endler, J.A. (1990) On the measurement and classification of colour in studies of animal colour patterns. *Biological Journal of the Linnean Society*, 41(4), 315–352. Available from: <https://doi.org/10.1111/j.1095-8312.1990.tb00839.x>
- Endler, J.A. (2012) A framework for analysing colour pattern geometry: adjacent colours. *Biological Journal of the Linnean Society*, 107(2), 233–253. Available from: <https://doi.org/10.1111/j.1095-8312.2012.01937.x>
- Endler, J.A., Cole, G.L. & Kranz, A.M. (2018) Boundary strength analysis: combining colour pattern geometry and coloured patch visual properties for use in predicting behaviour and fitness. *Methods in Ecology and Evolution*, 9(12), 2334–2348. Available from: <https://doi.org/10.1111/2041-210X.13073>
- Endler, J.A. & Houde, A.E. (1995) Geographic variation in female preferences for male traits in *poecilia reticulata*. *Evolution*, 49(3), 456–468. Available from: <https://doi.org/10.1111/j.1558-5646.1995.tb02278.x>
- Endler, J.A. & Mielke, P.W. (2005) Comparing entire colour patterns as birds see them. *Biological Journal of the Linnean Society*, 86(4), 405–431. Available from: <https://doi.org/10.1111/j.1095-8312.2005.00540.x>
- Endler, J.A., Westcott, D.A., Madden, J.R. & Robson, T. (2005) Animal visual systems and the evolution of color patterns: sensory processing illuminates signal evolution. *Evolution*, 59(8), 1795–1818.
- Ezray, B.D., Wham, D.C., Hill, C.E. & Hines, H.M. (2019) Unsupervised machine learning reveals mimicry complexes in bumblebees occur along a perceptual continuum. *Proceedings of the Royal Society B: Biological Sciences*, 286(1910), 20191501. Available from: <https://doi.org/10.1098/rspb.2019.1501>
- Gante, H.F., Matschiner, M., Malmström, M., Jakobsen, K.S., Jentoft, S. & Salzburger, W. (2016) Genomics of speciation and introgression in princess cichlid fishes from Lake Tanganyika. *Molecular Ecology*, 25(24), 6143–6161. Available from: <https://doi.org/10.1111/mec.13767>
- Gautier, M., Yamaguchi, J., Foucaud, J., Loiseau, A., Ausset, A., Facon, B. et al. (2018) The genomic basis of color pattern polymorphism in the harlequin ladybird. *Current Biology*, 28(20), 3296–3302, e7. Available from: <https://doi.org/10.1016/j.cub.2018.08.023>
- Gollapudi, S. (2019) OpenCV with python. In: Gollapudi, S. (Ed.) *Learn computer vision using OpenCV*. Berkeley, CA, USA: Apress, pp. 31–50. Available from: [https://doi.org/10.1007/978-1-4842-4261-2\\_2](https://doi.org/10.1007/978-1-4842-4261-2_2)
- Graham, C.H. & Hsia, Y. (1958) Color defect and color theory: studies of normal and color-blind persons, including a subject color-blind in one eye but not in the other. *Science*, 127(3300), 675–682.
- Guth, S.L., Alexander, J.V., Chumley, J.I., Gillman, C.B. & Patterson, M.M. (1968) Factors affecting luminance additivity at threshold among normal and color-blind subjects and elaborations of a trichromatic-opponent colors theory. *Vision Research*, 8(7), 913–928. Available from: [https://doi.org/10.1016/0042-6989\(68\)90140-5](https://doi.org/10.1016/0042-6989(68)90140-5)
- Hartigan, J.A. & Wong, M.A. (1979) Algorithm AS 136: a k-means clustering algorithm. *Journal of the Royal Statistical Society: Series C: Applied Statistics*, 28(1), 100–108.
- Hofmann, C.M., O'Quin, K.E., Marshall, N.J., Cronin, T.W., Seehausen, O. & Carleton, K.L. (2009) The eyes have it: regulatory and structural changes both underlie cichlid visual pigment diversity. *PLoS Biology*, 7(12), e1000266.
- Hooper, S.E., Weller, H. & Amelon, S.K. (2020) Countcolors, an R package for quantification of the fluorescence emitted by *Pseudogymnoascus destructans* lesions on the wing membranes of hibernating bats. *Journal of Wildlife Diseases*, 56(4), 759–767.
- Houde, A.E. & Torio, A.J. (1992) Effect of parasitic infection on male color pattern and female choice in guppies. *Behavioral Ecology*, 3(4), 346–351. Available from: <https://doi.org/10.1093/beheco/3.4.346>
- Janos, S. (Ed.). (2007) *Colorimetry: understanding the CIE system* (3rd ed). Comm. Internat. de l'éclairage.
- Johnsen, S. (2016) How to measure color using spectrometers and calibrated photographs. *Journal of Experimental Biology*, 219(6), 772–778. Available from: <https://doi.org/10.1242/jeb.124008>
- Jonathan, B.B. (1977) A unity underlying the different zebra striping patterns. *Journal of Zoology*, 183(4), 527–539.
- Karagic, N., Härer, A., Meyer, A. & Torres-Dowdall, J. (2018) Heterochronic opsin expression due to early light deprivation results in drastically shifted visual sensitivity in a cichlid fish: possible role of thyroid hormone signaling. *Journal of Experimental Zoology Part B: Molecular and Developmental Evolution*, 330(4), 202–214.
- Kohda, M., Jordan, L.A., Hotta, T., Kosaka, N., Karino, K., Tanaka, H. et al. (2015) Facial recognition in a group-living cichlid fish. *PLoS One*, 10(11), e0142552. Available from: <https://doi.org/10.1371/journal.pone.0142552>
- Kondo, S. & Asai, R. (1995) A reaction–diffusion wave on the skin of the marine angelfish Pomacanthus. *Nature*, 376(6543), 765–768. Available from: <https://doi.org/10.1038/376765a0>
- Kratochwil, C.F., Liang, Y., Gerwin, J., Woltering, J.M., Urban, S., Henning, F. et al. (2018) Agouti-related peptide 2 facilitates convergent evolution of stripe patterns across cichlid fish radiations. *Science*, 362(6413), 457–460. Available from: <https://doi.org/10.1126/science.aoa6809>
- Kratochwil, C.F. & Mallarino, R. (2023) Mechanisms underlying the formation and evolution of vertebrate color patterns. *Annual Review of Genetics*, 57, 135–156.
- Laitly, A., Callaghan, C.T., Delhey, K. & Cornwell, W.K. (2021) Is color data from citizen science photographs reliable for biodiversity research? *Ecology and Evolution*, 11(9), 4071–4083. Available from: <https://doi.org/10.1002/ece3.7307>
- Laurence-Chasen, J., Manafzadeh, A.R., Hatsopoulos, N.G., Ross, C.F. & Arce-McShane, F.I. (2020) Integrating XMALab and DeepLabCut for high-throughput XROMM. *Journal of Experimental Biology*, 223(17), jeb226720.
- Leite, T.S. & Mather, J.A. (2008) A new approach to octopuses' body pattern analysis: a framework for taxonomy and behavioral studies. *American Malacological Bulletin*, 24(1), 31–41.
- Liang, Y., Gerwin, J., Meyer, A. & Kratochwil, C.F. (2020) Developmental and cellular basis of vertical bar color patterns in the east African cichlid fish *Haplochromis latifasciatus*. *Frontiers in Cell and Developmental Biology*, 8, 62. Available from: <https://doi.org/10.3389/fcell.2020.00062>
- Maia, R., Gruson, H., Endler, J.A. & White, T.E. (2019) Pavo 2: new tools for the spectral and spatial analysis of colour in R. *Methods in Ecology and Evolution*, 10(7), 1097–1107.
- Marchini, M., Sommaggio, D. & Minelli, A. (2017) Playing with black and yellow: the evolvability of a Batesian mimicry. *Evolutionary Biology*, 44(1), 100–112. Available from: <https://doi.org/10.1007/s11692-016-9397-0>
- Mason, N.A. & Bowie, R.C.K. (2020) Plumage patterns: ecological functions, evolutionary origins, and advances in quantification. *The Auk*, 137(4), ukaa060. Available from: <https://doi.org/10.1093/auk/ukaa060>
- Mathis, A., Mamidanna, P., Cury, K.M., Abe, T., Murthy, V.N., Mathis, M.W. et al. (2018) DeepLabCut: Markerless pose estimation of user-defined body parts with deep learning. *Nature Neuroscience*, 21(9), 1281–1289.

- MathWorks. (2023) *MATLAB and image processing toolbox (version 2023a)* [MATLAB]. The Mathworks Inc. <https://www.mathworks.com/help/images/>
- Medina, I., Wang, I.J., Salazar, C. & Amézquita, A. (2013) Hybridization promotes color polymorphism in the aposematic harlequin poison frog, *Oophaga histrionica*. *Ecology and Evolution*, 3(13), 4388–4400. Available from: <https://doi.org/10.1002/ece3.794>
- Megía-Palma, R., Martínez, J. & Merino, S. (2018) Manipulation of parasite load induces significant changes in the structural-based throat color of male Iberian green lizards. *Current Zoology*, 64(3), 293–302.
- Menychtas, D., Petrou, N., Kansizoglu, I., Giannakou, E., Grekidas, A., Gasteratos, A. et al. (2023) Gait analysis comparison between manual marking, 2D pose estimation algorithms, and 3D marker-based system. *Frontiers in Rehabilitation Sciences*, 4, 1238134. Available from: <https://doi.org/10.3389/fresc.2023.1238134>
- Miyazawa, S. (2020) Pattern blending enriches the diversity of animal colorations. *Science Advances*, 6(49), eabb9107. Available from: <https://doi.org/10.1126/sciadv.eabb9107>
- Miyazawa, S., Okamoto, M. & Kondo, S. (2010) Blending of animal colour patterns by hybridization. *Nature Communications*, 1(1), 66. Available from: <https://doi.org/10.1038/ncomms1071>
- Mouselimis, L. (2023) *OpenImageR: an image processing toolkit*. <https://CRAN.R-project.org/package=OpenImageR>
- Neave, F., Mandrak, N., Docker, M. & Noakes, D. (2006) Effects of preservation on pigmentation and length measurements in larval lampreys. *Journal of Fish Biology*, 68(4), 991–1001.
- Nugent, J. (2018) iNaturalist. *Science Scope*, 41(7), 12–13.
- Ooms, J. (2023) *Magick: advanced graphics and image-processing in R*. <https://docs.ropensci.org/magick/> <https://ropensci.r-universe.dev/magick>
- Orteu, A. & Jiggins, C.D. (2020) The genomics of coloration provides insights into adaptive evolution. *Nature Reviews Genetics*, 21(8), 461–475. Available from: <https://doi.org/10.1038/s41576-020-0234-z>
- Parham, J., Stewart, C., Crall, J., Rubenstein, D., Holmberg, J. & Berger-Wolf, T. (2018) An animal detection pipeline for identification. *IEEE Winter Conference on Applications of Computer Vision (WACV)*, 2018, 1075–1083. Available from: <https://doi.org/10.1109/WACV.2018.00123>
- Poll, M. (1974) Contribution à la faune ichthyologique du lac Tanganyika, d'après les récoltes de P. Brichard. *Revue de Zoologie africaine*, 88, 99–110.
- Poulsen, J.Y., Sado, T., Hahn, C., Byrkjedal, I., Moku, M. & Miya, M. (2016) Preservation obscures pelagic deep-sea fish diversity: doubling the number of sole-bearing opisthoproctids and resurrection of the genus Monacoa (Opisthoproctidae, Argentiniformes). *PLoS One*, 11(8), e0159762.
- Poulton, E.B. (1890) *The Colours of animals: their meaning and use, especially considered in the case of insects*. D. Appleton. <https://books.google.com/books?id=Uf4vAAAAYAAJ>
- R Core Team. (2022) *R: a language and environment for statistical computing*. R Foundation for Statistical Computing. <https://www.R-project.org/>
- Remsen, J., Jr. (1984) High incidence of “leapfrog” pattern of geographic variation in Andean birds: implications for the speciation process. *Science*, 224(4645), 171–173.
- Ressel, S. & Schall, J.J. (1989) Parasites and showy males: malarial infection and color variation in fence lizards. *Oecologia*, 78(2), 158–164. Available from: <https://doi.org/10.1007/BF00377151>
- Robinson, M.L., Weber, M.G., Freedman, M.G., Jordan, E., Ashlock, S.R., Yonenaga, J. et al. (2023) Macroevolution of protective coloration across caterpillars reflects relationships with host plants. *Proceedings of the Royal Society B: Biological Sciences*, 290(1991), 20222293. Available from: <https://doi.org/10.1098/rspb.2022.2293>
- Santos, M.E., Baldo, L., Gu, L., Boileau, N., Musilova, Z. & Salzburger, W. (2016) Comparative transcriptomics of anal fin pigmentation patterns in cichlid fishes. *BMC Genomics*, 17(1), 712. Available from: <https://doi.org/10.1186/s12864-016-3046-y>
- Saysani, A., Corballis, M.C. & Corballis, P.M. (2018) The colour of words: How dichromats construct a colour space. *Visual Cognition*, 26(8), 601–607.
- Schneider, C.A., Rasband, W.S. & Eliceiri, K.W. (2012) NIH image to ImageJ: 25 years of image analysis. *Nature Methods*, 9(7), 671–675.
- Schwartz, S.T. & Alfaro, M.E. (2021) Sashimi: a toolkit for facilitating high-throughput organismal image segmentation using deep learning. *Methods in Ecology and Evolution*, 12(12), 2341–2354.
- Sheehan, M.J., Choo, J. & Tibbetts, E.A. (2017) Heritable variation in colour patterns mediating individual recognition. *Royal Society Open Science*, 4(2), 161008.
- Stevens, M., Párraga, C.A., Cuthill, I.C., Partridge, J.C. & Troscianko, T.S. (2007) Using digital photography to study animal coloration. *Biological Journal of the Linnean Society*, 90(2), 211–237. Available from: <https://doi.org/10.1111/j.1095-8312.2007.00725.x>
- Stockman, A. & Sharpe, L.T. (2000) The spectral sensitivities of the middle-and long-wavelength-sensitive cones derived from measurements in observers of known genotype. *Vision Research*, 40(13), 1711–1737.
- Stuckert, A.M.M., Chouteau, M., McClure, M., LaPolice, T.M., Linderoth, T., Nielsen, R. et al. (2021) The genomics of mimicry: gene expression throughout development provides insights into convergent and divergent phenotypes in a Müllerian mimicry system. *Molecular Ecology*, 30(16), 4039–4061. Available from: <https://doi.org/10.1111/mec.16024>
- Tea, Y.-K., Hobbs, J.-P.A., Vitelli, F., DiBattista, J.D., Ho, S.Y.W. & Lo, N. (2020) Angels in disguise: sympatric hybridization in the marine angelfishes is widespread and occurs between deeply divergent lineages. *Proceedings of the Royal Society B: Biological Sciences*, 287(1932), 20201459. Available from: <https://doi.org/10.1098/rspb.2020.1459>
- Trewavas, E. & Poll, M. (1952) Three new species and two new subspecies of the genus Lamprologus, cichlid fishes of Lake Tanganyika. *Bulletin du Musée Royal d'Histoire Naturelle de Belgique*, 28(50), 1–16.
- Troscianko, J. & Stevens, M. (2015) Image calibration and analysis toolbox—a free software suite for objectively measuring reflectance, colour and pattern. *Methods in Ecology and Evolution*, 6(11), 1320–1331. Available from: <https://doi.org/10.1111/2041-210X.12439>
- Tumulty, J.P., Miller, S.E., Van Belleghem, S.M., Weller, H.I., Jernigan, C.M., Vincent, S. et al. (2023) Evidence for a selective link between cooperation and individual recognition. *Current Biology*, S0960982223015828, 5478–5487. Available from: <https://doi.org/10.1016/j.cub.2023.11.032> e5.
- Van Belleghem, S.M., Alicea Roman, P.A., Carbia Gutierrez, H., Counterman, B.A. & Papa, R. (2020) Perfect mimicry between *Heliconius* butterflies is constrained by genetics and development. *Proceedings of the Royal Society B*, 287(1931), 20201267.
- Van Belleghem, S.M., Papa, R., Ortiz-Zuazaga, H., Hendrickx, F., Jiggins, C.D., Owen McMillan, W. et al. (2018) Patternize: an R package for quantifying colour pattern variation. *Methods in Ecology and Evolution*, 9(2), 390–398. Available from: <https://doi.org/10.1111/2041-210X.12853>
- Van Den Berg, C.P., Endler, J.A. & Cheney, K.L. (2023) Signal detectability and boldness are not the same: the function of defensive coloration in nudibranchs is distance-dependent. *Proceedings of the Royal Society B: Biological Sciences*, 290(2003), 20231160. Available from: <https://doi.org/10.1098/rspb.2023.1160>
- van den Berg, C.P., Troscianko, J., Endler, J.A., Marshall, N.J. & Cheney, K.L. (2020) Quantitative colour pattern analysis

- (QCPA): a comprehensive framework for the analysis of colour patterns in nature. *Methods in Ecology and Evolution*, 11(2), 316–332. Available from: <https://doi.org/10.1111/2041-210X.13328>
- Vorobyev, M. & Osorio, D. (1998) Receptor noise as a determinant of colour thresholds. *Proceedings of the Royal Society of London. Series B: Biological Sciences*, 265(1394), 351–358.
- Vuilleumier, F. (1969) Pleistocene speciation in birds living in the high Andes. *Nature*, 223(5211), 1179–1180.
- Wickham, H., Hester, J., Chang, W. & Hester, M.J. (2021) *Package ‘devtools’*.
- Winters, A.E., Wilson, N.G., Van Den Berg, C.P., How, M.J., Endler, J.A., Marshall, N.J. et al. (2018) Toxicity and taste: unequal chemical defences in a mimicry ring. *Proceedings of the Royal Society B: Biological Sciences*, 285(1880), 20180457. Available from: <https://doi.org/10.1098/rspb.2018.0457>
- Zhou, B. (2015) Image segmentation using SLIC superpixels and affinity propagation clustering. *International Journal of Scientific Research*, 4(4), 1525–1529.

## SUPPORTING INFORMATION

Additional supporting information can be found online in the Supporting Information section at the end of this article.

**How to cite this article:** Weller, H.I., Hiller, A.E., Lord, N.P. & Van Belleghem, S.M. (2024) recolorize: An R package for flexible colour segmentation of biological images. *Ecology Letters*, 27, e14378. Available from: <https://doi.org/10.1111/ele.14378>